Egypt.J.Chem. **Vol. 62**, No. 5. pp. 811 - 825 (2019)

Egyptian Journal of Chemistry

http://ejchem.journals.ekb.eg/

Mitigation of Hydrogen Evolution During Zinc Corrosion in Aqueous Acidic Media Using 5-Amino-4-imidazolecarboxamide

S. Abd El Wanees[1, 2, *], M. I. Alahmdi[1], M. A.Alsharif[1], Y. Atef[3]

[1]*Chemistry Department, Faculty of Science, University of Tabuk, Tabuk, Saudi Arabia.*

[2]*Chemistry Department, Faculty of Science, Zagazig University, Zagazig, 44519, Egypt.*

[3]*Chemistry Administration, Cairo, Egypt.*

THE rate of H_2 production was investigated during the dissolution of Zn in 0.5 M HCl in the absence and presence different concentrations of 5-amino-4-imidazolecarboxamide (AIC). Different techniques such as gasometry, electrochemical and scanning electron microscope are used. The data indicated that the rate of hydrogen evolution was increased with the inundation time and temperature and was mitigated with the presence of AIC inhibitor. The electrochemical impedance spectroscopy showed that AIC introduced an inhibitive film that can control the rate of corrosion of zinc. Polarization data indicated that AIC acted as a surface-active molecule that behaves as a mixed-type inhibitor. The free energy of adsorption and adsorption-desorption equilibrium constants were deduced and discussed.

Keywords: Imidazole, Zinc, Corrosion inhibition, Hydrogen production, Potentiodynamic, Adsorption.

Introduction

Zn and zinc alloys are used in many applications, among which the chargeable batteries and steel galvanization for corrosion protection [1-4]. The importance of the corrosion study of Zinc and its alloys comes from the feasibility of production of hydrogen when these materials allowed being in contact with dilute acids [5-7]. Logically, this idea is important to produce hydrogen, avoiding storing problems, as a fuel used for operating fuel cells, as a sustainable alternative to energy. This idea deserves attention to the production of fresh hydrogen used in the operation of fuel cells without the need for a storage phase to avoid storage problems.

Organic bulky molecules containing heteroatoms such as O, S, N, P and unsaturated bonds are considered as effective inhibitors that can tolerate the metal dissolution process through an adsorption step [8-14]. The heteroatoms of inhibitor molecules are rich with lone pairs of free electrons, which are considered as active sites available for adsorption on the metal surface forming a protective layer that keeps the metal surface from the destructive effect of the surrounding media.

Among the several classes of organic compounds, imidazole derivatives were found as better inhibitors against corrosion for many metals and alloys in the aqueous solutions [15-20]. Imidazole and imidazolecarboxamide derivatives are classified as an important type of organic inhibitors. This is due to the presence of several N atoms, π- electrons of aromatic rings and the electronegative O atom of the carbonyl group that may be attached within the molecule [15-18] easy to adsorb on the metal to form a protective film. The inhibition activity of different types of inhibitors towards the corrosion of zinc and H_2 production in acidic media has been rarely investigated [17-22]. Therefore, the main goal is to evaluate 5-amino-4-imidazolecarboxamide (AIC) as a corrosion inhibitor towards the dissolution of Zn and

*Corresponding author e-mail: s_nasr@ut.edu.sa
Received 31/10/2018; Accepted 20/12/2018
DOI: 10.21608/EJCHEM.2018.6006.1507
©2019 National Information and Documentation Center (NIDOC)

controller for H_2 production in 0.5 M HCl solution. Chemical (gasometry) and electrochemical (Tafel and EIS) techniques, complemented by surface investigations using SEM techniques were used.

Experimental

Materials and electrolyte

Inhibitor preparation

Zinc sheet 99.99 % pure (Johnson- Matthey, UK) had been cut in coupons with dimensions 1.8, 3.7 and 0.3 cm for H_2 production study. For electrochemical studies, a Zn rod was used as a working electrode entrenched in a glass tube with an epoxy resin leaving an uncovered cross-section area of 0.32 cm^2. Before each run, the Zn specimen was mechanically polished using different grades of emery papers. The specimen washed by doubly distilled water and degreased with acetone before inundation in the acid solution. 5-Amino-4-imidazolecarboxamide (AIC), Merck, was used as an inhibitor for corrosion of zinc. All experiments were done at 25 ± 1°C, except those carried to investigate the effect of temperature on the corrosion rate.

A Zn sheet with purity 99.99 % (Johnson-Matthey, UK) was cut into similar samples with dimensions 2.0 cm x 5.0 cm x 0.3 cm which were used for hydrogen measurement. For the electrochemical method, a zinc rod (working electrode, *WE*) has the same chemical composition was entrenched in epoxy resin with the free surface area of 0.28 cm^2 was used. The Zn surface was, successively, abraded with different grades of fine emery papers up to mirror finish. Then, it was washed with bi-distilled water, followed by rinsing with a degreasing solvent, washed repeatedly with bi-distilled water, and finally immersed in the test solution. A fresh 0.5 M hydrochloric acid aqueous solution was prepared using 37% HCl (BDH) and bi-distilled water. The inhibitor concentrations varied between 1.0 x10^{-6} and 2.5 x10^{-5} M freshly prepared in 0.5 M HCl before running the experiment.

Experimental techniques

The volume of the collected H_2 gas was calculated per unit area of Zn specimen at different inundation times using gasometry apparatus as reported before [8, 21,22]. Potentiodynamic polarization and EIS study, under static conditions, at 25°C, were done using a Volta lab 80 (PGZ 402) potentiostat with Volta master 4 software. Three electrodes system consists of Zn rode as *WE*, a pure platinum sheet as an auxiliary electrode and a saturated calomel electrode as a reference electrode were used. The Zn electrode was immersed in the test solution for about 2 h before polarization and EIS measurements to establish steady-state potential, E_{st}. The *E-I* curves were obtained by sweeping the electrode potential in the potential range from ± 200 mV relative to the steady-state potential, E_{corr}. The corrosion current density, I_{corr} is performed by extrapolating the linear portions of the cathodic and anodic branches back to their intersection at E_{st}. Electrochemical impedance spectroscopy, EIS curves were obtained by employing a frequency range of 100 kHz to 0.1 Hz using a signal amplitude of 5 mV using AC signals at open circuit potential, E_{corr}.

Surface investigation

The surface morphology of some corroded Zn specimens (1 cm × 1 cm) was investigated before and after immersing for 2 hr in both uninhibited (0.5 M HCl) and inhibited (0.5 M HCl + 1x10^{-5} M AIC inhibitor) solutions using

TABLE 1. The inhibitor name, chemical structure, empirical formula and molecular weight.

Name	Chemical Structure	Empirical Formula	Molecular Weight
5-Amino-4-imidazole-carboxamide (AIC)	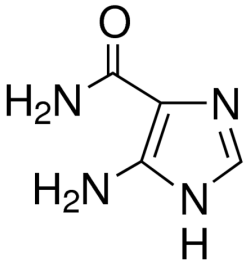	$C_4H_6N_4O$	126.12

scanning electron microscope, SEM. The used SEM was A Jeol type, JSM-5410 (Japan), with an accelerated voltage of 25 kV and a working distance of 20 mm was used.

Results and Discussion

Gasometry study

The inhibition effect of 5-amino-4-imidazolecarboxamide (AIC) towards the corrosion of Zn in HCl, was investigated through the variation in the volume of the evolved hydrogen gas (V) with the inundation time, t. Figure 1 depicted V-t curves of Zn in 0.5 M HCl solutions without and with various additives of AIC, at 25°C. The decrease in the volume of the evolved H_2 gas in presence of AIC inhibitor is due to the reduction in the corrosion process. The rate of the H_2 gas production can be determined from the slope of the V-t relation [23, 24]. It is clear that the H_2 gas initiates to evolve after an incubation period, at which the protective passive film is destroyed by the effect of Cl^- ions [24]. The incubation period is increased as the AIC inhibitor concentration

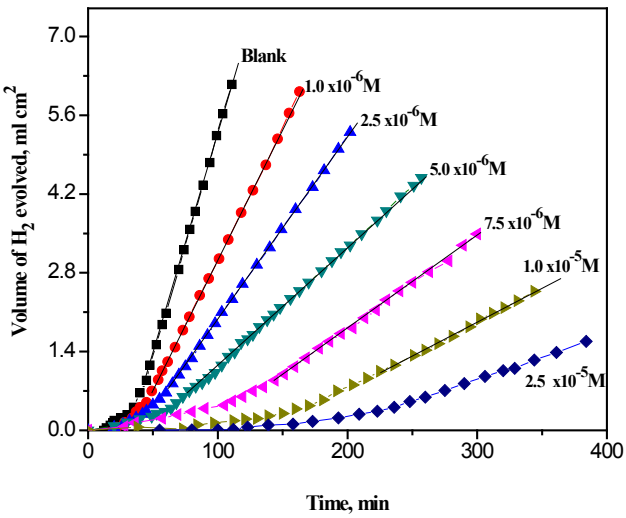

Fig. 1. Variation of the volume of H_2 gas evolved with the immersion time for Zn in 0.5 M HCl devoid of and containing different additions of AIC, at 25 °C.

is increased. Such behavior would confirm the presence of a protective film. On the other hand, the rise in the temperature will shortage the incubation period due to a corrosion acceleration effect [25].

The variation in the rate of H_2 production, r_{corr} with log C_{inh}, at different temperatures is shown in Fig. 2. It is clear that the decrease in r_{corr} with log C_{inh} shows a sigmoid S-curve relation. Such behavior is similar to an adsorption isotherm which indicate that AIC inhibitor could be adsorbed on Zn surface decreasing the corrosion rate of Zn [23, 24].

The surface coverage, θ, and the inhibition efficiency, η % are calculated from the corrosion rate values in the absence and presence of the inhibitor solution, r_{corr} and r'_{corr}, respectively, according to the following equations [24-27]:

$$\theta = \left(\frac{r_{corr} - r'_{corr}}{r_{corr}}\right) \quad (1)$$

$$\eta\% = \left(\frac{r_{corr} - r'_{corr}}{r_{corr}}\right)100 \quad (2)$$

The values of θ and η % at different concentrations of AIC are included in Table 2. These values are increased with increasing the concentration of AIC and are decreased with rising the solution temperature. Such data confirms the adsorption-desorption of AIC molecules on Zn surface, at higher temperatures, which proves the physically adsorbed mechanism [28].

Polarization study

The anodic-cathodic potentiodynamic polarization curves of Zn in 0.5 M HCl solution without and with various additions of AIC, at 298K are depicted in Fig. 3. It is noted that the corrosion current densities are reduced in the presence of AIC due to an overvoltage

TABLE 2. Values of corrosion rate, r_{corr} (ml cm^{-2}min^{-1}), surface coverage, θ, and inhibition efficiency, η %, of different concentrations of AIC for corrosion of Zn in 0.5 M HCl, at different temperatures.

K	property	Concentration, M						
		Free	1.0x10^{-6}	2.5x10^{-6}	5.0x10^{-6}	7.5x10^{-6}	1.0x10^{-5}	2.5x10^{-5}
298	r_{corr}	0.080	0.047	0.033	0.021	0.016	0.012	0.008
	θ	--	0.42	0.59	0.73	0.80	0.85	0.90
	η%	--	41.80	59.30	73.30	79.80	85.40	90.40
308	r_{corr}	0.087	0.057	0.040	0.028	0.022	0.019	0.013
	θ	--	0.34	0.53	0.68	0.75	0.79	0.86
	η%	--	34.00	53.20	68.00	75.30	78.70	85.60
318	r_{corr}	0.099	0.068	0.049	0.034	0.029	0.026	0.018
	θ	---	0.24	0.40	0.56	0.64	0.71	0.82
	η%	--	23.90	40.40	55.70	64.00	71.00	82.00
328	r_{corr}	0.115	0.084	0.063	0.044	0.039	0.034	0.024
	θ	--	0.27	0.45	0.62	0.66	0.71	0.79
	η%	--	26.96	45.22	61.74	66.26	70.70	79.39

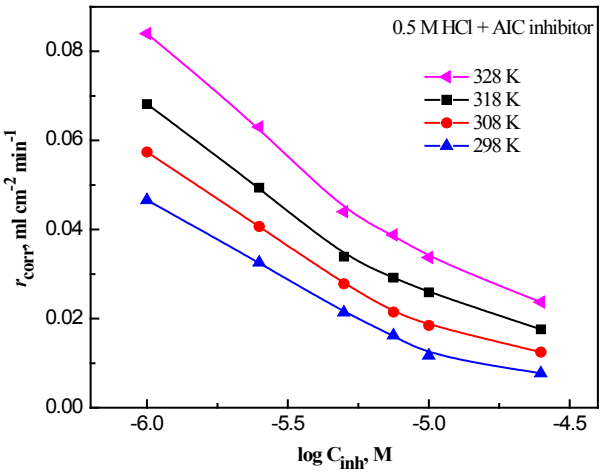

Fig. 2. Variation in the rate of H_2 gas production, r_{corr}, with the logarithm of AIC concentration, at different temperatures.

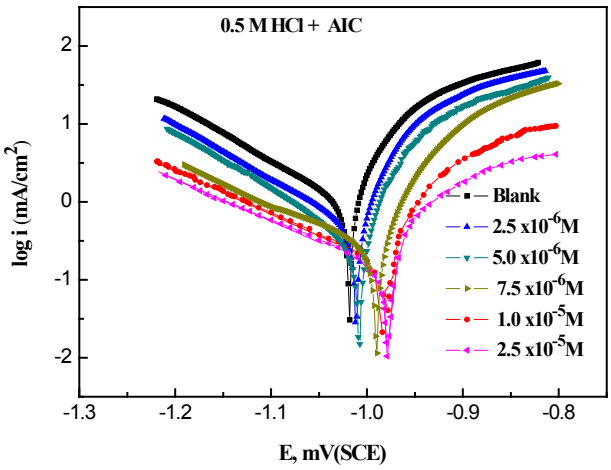

Fig. 3. E-log i curves of zinc in 0.5 M HCl solution in the absence and presence of different concentrations of AIC, at 298 K.

accompanying each of the anodic and cathodic processes. This behavior could prove that the mechanism of Zn dissolution and H_2 production are under activation-controlled process, and not altered by the presence of inhibitor [28, 29].

The values of the corrosion current densities in the absence, I°_{corr}, and presence of AIC inhibitor, I_{corr}, are used to calculate the surface coverage, θ, and the inhibition efficiency η' %, respectively, according to the following equations [25-29].

$$\theta = \left(\frac{I^{\circ}_{corr} - I_{corr}}{I^{\circ}_{corr}}\right) \quad (3)$$

$$\eta'\% = \left(\frac{I^{\circ}_{corr} - I_{corr}}{I^{\circ}_{corr}}\right)100 \quad (4)$$

The data of steady-state potential, E_{corr}, I_{corr}, anodic and cathodic Tafel slopes (β_a & β_c), θ and η'% are tabulated in Table 3. It is noted that I_{corr} is lowered while each of θ and η'% are increased with AIC concentration due to the inhibitive effect of AIC towards the corrosion of Zn.

TABLE 3. Potentiodynamic polarization parameters for the corrosion of Zn in 0.5 M HCl containing different concentrations of AIC, at 298 K.

Conc, M	- E_{corr}, mV	I_{corr}, mAcm^{-2}	-β_c mV/dec	B_a, mV/dec,	ή%
Blank	1018	0.77	131	41.6	--
2.5x10^{-6}	1011	0.42	135	41	45.46
5.0x10^{-6}	1006	0.30	122	39	66.24
7.5x10^{-6}	1989	0.24	136	34	71.43
1.0x10^{-5}	0984	0.14	120	37	83.12
2.5x10^{-5}	0978	0.08	123	36	89.61

In addition, the non-significant changes in the values of β_a and β_c, beside the little displacement in E_{corr} (6-30 mV$_{SCE}$), which is < 85 mV; confirm that AIC molecules behaved as a mixed inhibitor [30-35].

Electrochemical impedance spectroscopy measurements

Figure 4 depicted the Nyquist diagrams of Zn in 0.5 M HCl without and with different concentrations of AIC inhibitor. The Nyquist plots show a single depressed capacitive semicircle for both blank and AIC inhibitor solutions. The depressed semicircles, which probably correspond to Nyquist diagrams is characteristic of solid electrodes that exhibit frequency dispersion due to the roughness and other inhomogeneity of the metal surface [29]. The single semicircular capacitive loop is considered as an indication of a single charge transfer process controlling the Zn corrosion reaction [29]. This shape was unaffected in the presence of AIC at different concentrations revealing that the corrosion process has an activation-controlled nature does not change, in agreement with polarization investigation [29, 36]. The centers of these depressed loops were displaced below the real axis. This phenomenon may be related to the frequency dispersion. Such behavior could be referred to the frequency dispersion influence of the interfacial impedance and the inhomogeneous Zn surface [37]. It is ordinarily attributed to the presence of coarseness roughness and inhibitor adsorption [38, 39]. Moreover, the presence of AIC inhibitor increased the diameter of the capacitive loops than that of free HCl solution, that the surface of zinc metal is covered by a barrier film in presence of AIC inhibitor and impedes the corrosion of Zn [38].

The impedance spectra are investigated by fitting the experimental data to the equivalent circuit as given in Fig. 5. The impedance parameters like the charge transfer resistance (R_{ct}), the solution resistance (R_s), double layer capacitance, C_{dl}, and percentage inhibition efficiency (η" %) are represented in Table 4. it is obvious that R_{ct} and η" % values are increased with AIC concentration confirming the formation of a protective film on the metal/solution interface [39, 40]. The values of electrical double layer capacitance, C_{dl}, was inversely proportional with R_{ct} according to the relation:

$$C_{dl} = \left(\frac{1}{2\pi f_{max}}\right)\left(\frac{1}{R_{ct}}\right) \quad (5)$$

where f_{max} is the frequency at maximum imaginary impedance.

The values of C_{dl} were reduced in presence of AIC inhibitor (Table 4), due to the rise in the intensity of the electrical double layer around the protective film and/or decrease the local dielectric constant due to the permutation of H_2O molecules at the Zn surface by the adsorbed AIC molecules [39].

Also, the reduction in C_{dl} values in presence of AIC is inversely proportional to the double layer thickness, δ, according to Helmholtz model [40, 41].

$$C_{dl} = \left(\frac{\varepsilon\varepsilon^{\circ}S}{\delta}\right) \quad (6)$$

where ε is the dielectric constant, S is the electrode surface area and ε° is the air permittivity. The lower values of C_{dl} with higher additions of AIC inhibitor may be attributed to the efficacious adsorption process. This fact suggests that the inhibitor molecules could firstly be adsorbed on Zn surface, covering the active sites.

The values of inhibition efficiencies, η" %, (Table 4), are obtained from R_{ct} values using the equation [35]:

$$\eta''\% = \left(\frac{R_{ct} - R'_{ct}}{R_{ct}}\right) 100 \quad (7)$$

where R_{ct} and R'_{ct} are the electric charge transfer resistance for Zn in 0.5 M HCl with and without AIC, respectively. The values of η" % increase with the rise in the AIC concentrations to reach a maximum efficiency (76.8 %) at 2.5×10^{-5} M. The above results indicate that with an increase in AIC concentration a more protective film is formed on the Zn surface. These data confirm the agreement between the results obtained by EIS and other techniques.

Temperature study

The study of temperature on the dissolution of Zn in 0.5 M HCl in the absence and presence of different concentrations of AIC inhibitor is used to determine the rate of hydrogen production, r_{corr} at different temperatures by gasometric

TABLE 4. EIs parameters for the corrosion of Zn in 0.5 M HCl containing different concentrations of AIC, at 298 K.

Conc, M	R_{ct}, (Ω.cm²)	R_s, (Ω.cm²)	C_{dl}, (μF/cm²)	θ	η" %
0.00	5.76	2.17	38.67	-----	------
2.5×10^{-6}	7.35	2.22	27.55	0.22	21.60
5.0×10^{-6}	13.00	2.18	20.33	0.53	55.70
7.5×10^{-6}	20.50	3.29	18.87	0.72	71.90
1.0×10^{-5}	24.91	3.44	17.45	0.77	76.90
2.5×10^{-5}	36.00	3.19	18.88	0.84	84.00

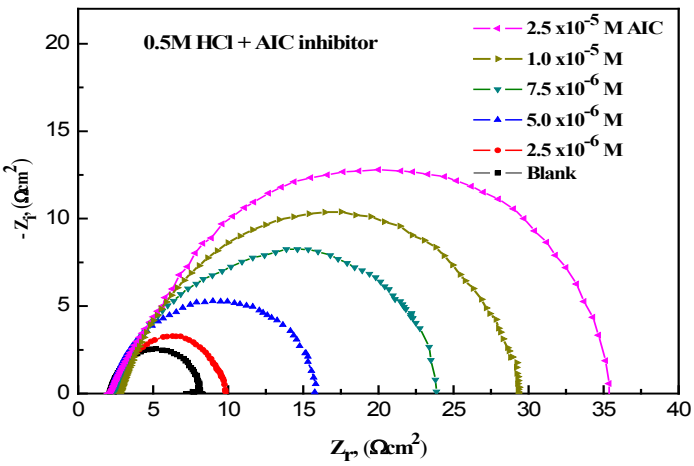

Fig. 4. EIS Nyquist for Zinc in 0.5 M HCl in the absence and presence of different concentrations of AIC, at 298 K.

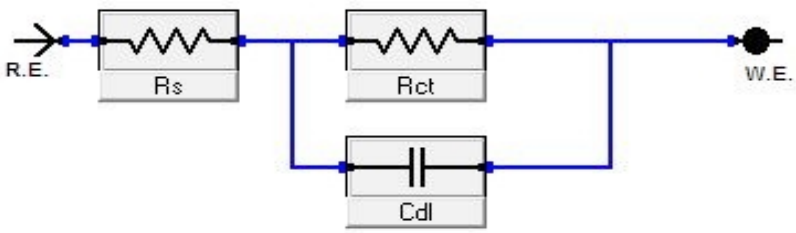

Fig. 5. Equivalent circuit model used for simulation of impedance spectra.

technique. The data indicated that the value of r_{corr} at different concentrations of AIC inhibitor was increased with a rise in temperature. Temperature accelerates the rate of H^+ ions diffusion and enhances the rate of H_2 production [42]. The relatively lower values of r_{corr}, in case of AIC inhibitor, establishes the mitigation of H_2 production, without altering the mechanism of the dissolution reaction.

The apparent activation energy, E_a, required for the dissolution of zinc metal and production of H_2 gas can be calculated using Arrhenius equation [42, 43]:

$$r_{corr} = A\exp\left(\frac{-E_a}{RT}\right) \quad (8)$$

where r_{corr} is the rate of hydrogen production, A represents the Arrhenius factor, T is the absolute temperature and $R = 8.314$ J mol^{-1} is the universal gas constant.

Plotting of log r_{corr} against T^{-1} in case of free 0.5 M HCl and 0.5 M HCl containing different concentrations of AIC inhibitor is depicted in Fig. 6. The obtained plots gave straight lines relation, which confirms Arrhenius equation. The activation energies E_a, were evaluated from the slope of the straight-line plots. The calculated values of activation energy are listed in Table 5. The obtained value of E_a for Zn in the blank solution is 11.40 kJ/mol. In presence of AIC inhibitor, E_a varied between 15.72 and 29.45 kJ/mol according to the inhibitor concentration. The increase in the values of E_a in presence of AIC inhibitor may be attributed to the presence of inhibitive film formed from AIC molecules on the zinc metal surface [44-46]. This observation further supports the physisorption mechanism [42, 47]. Further inspection of Table 5 also revealed that E_a increases with increase in the AIC inhibitor concentration, which supports the physical adsorption mechanism [42].

The values of r_{corr} (ml^{-1}cm^{-2}min^{-1}) at different temperatures are used to locate the values of apparent enthalpy, ΔH_a and entropy, ΔS_a of activation for the formation of the activation complex, using the following equation [42-45]:

$$r_{corr} = \frac{RT}{Nh}\exp\left(\frac{\Delta S_a}{R}\right)\exp\left(\frac{-\Delta H_a}{RT}\right) \quad (9)$$

where R is the universal gas constant, N is the Avogadro's number and h is Planck's constant. From the linear plot of log (r_{corr}/T) vs T^{-1}, (Fig. 7), ΔH_a and ΔS_a were calculated using the slope and the intercept values, successively, (Table 4). The positive sign of ΔH_a reflects the endothermic nature of Zn dissolution in the free acid and inhibitive solutions. The rise in the ΔH_a in case of AIC confirms the difficulty of Zn dissolution process in presence of AIC inhibitor [42]. The negative sign of ΔS_a (Table 5) suggests that the activated complex in the rate-determining step demonstrates a combination rather than a dissociation step, supporting a lessening in disorder happens through the transition state where the reactants changed to the activated complex [47]

Adsorption behavior

The adsorption of inhibitor molecules at the corroded metal surface in aqueous solutions can be attributed to the presence of some of the surface-active centers rich with free electrons. A substitution process during the adsorption where a reciprocation between adsorbed H_2O molecules and inhibitor molecules occurs.

The surface coverage, θ, appreciated from the data of gasometry measurements is used as a function of inhibitor concentration, to investigate the type of adsorption isotherm. The isotherm accounts for the nature of the interaction between the metal and inhibitor molecules. In our study,

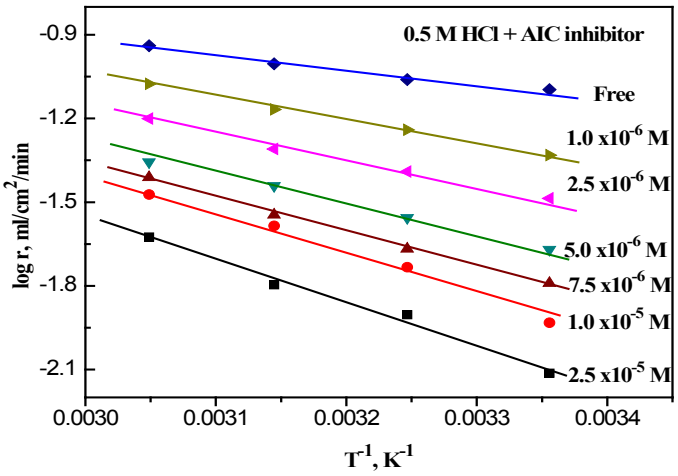

Fig. 6. Arrhenius plots variation of log r_{corr} against T^{-1}, for Zn in 0.5 M HCl devoid of and containing different concentrations of AIC.

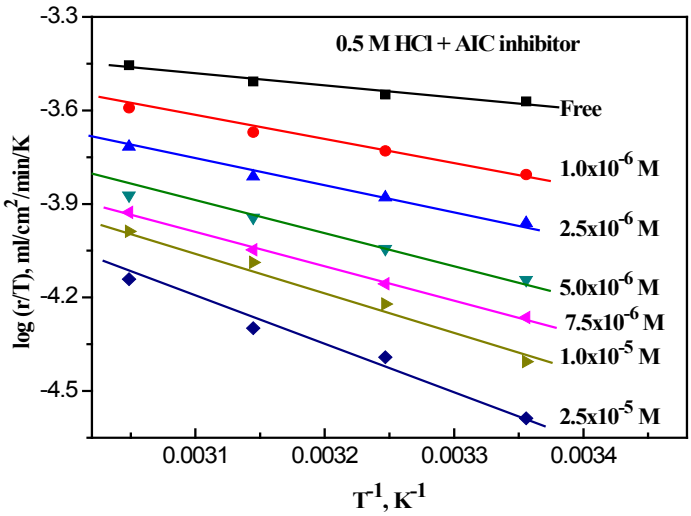

Fig. 7. Transition state plots, variation of log rcorr/T against T-1, for Zn in 0.5 M HCl devoid of and containing different concentrations of AIC.

TABLE 5. The values of the linear correlation coefficient, r, E_a, ΔH_a, ΔS_a for Zn in 0.5 M HCl without and with additions of AIC.

Inhibitor	r^2	E_a, kJmol^{-1}	ΔH_a, kJmol^{-1}	ΔS_a, Jmol^{-1}
Blank	0.990	11.4	7.26	-242
1.0x10^{-6}	0.999	15.72	13.13	-238
2.5x10^{-6}	0.999	18.30	14.93	-223
5.0x10^{-6}	0.998	20.70	18.13	-228
7.5x10^{-6}	0.998	23.55	20.97	-209
1.0x10^{-5}	0.959	28.64	25.85	-206
2.5x10^{-5}	0.999	29.45	27.19	-195

the best-fit isotherm was Langmuir-model. The applicable model can be achieved from the relation [43]:

$$\frac{C_{inh}}{\theta} = \frac{1}{K_{ads}} + C_{inh} \quad (10)$$

Experimental results of C_{inh}/θ vs C_{inh}, at different temperatures, give straight lines, as shown in Fig. 8. The obtained correlation coefficient (r^2 > 0.99) confirms this type of isotherm. The corresponding linear regression parameters including the linear correlation coefficient (r^2), slope, intercept and K_{ads} are collected in Table 5. The values of each of the slope and r are nearly equal one which confirms the adsorption of AIC on Zn surface follows to Langmuir's model. The higher values of K_{ads} for AIC inhibitor are consistent with the results of Morad when used other inhibitors for corrosion of Zn in acidic medium [48]. This reflects the interaction of the inhibitor with the metallic surface [48] confirming strong adsorption of

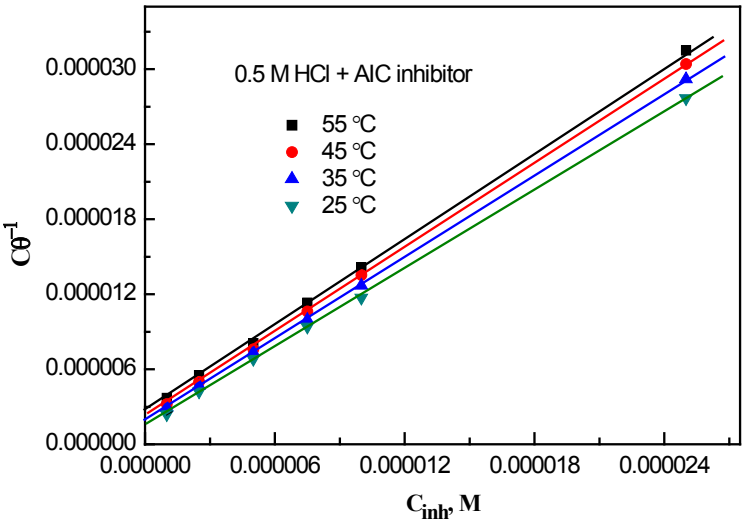

Fig. 8. Langmuir adsorption of AIC inhibitor on Zn in 0.5 M HCl, at different temperatures.

TABLE 6. The values of linear correlation coefficient, *r*, slope, intercept and K_{ads} for adsorption of AIC on Zn in 0.5M HCl, gasometry data.

Temperature, K	r^2	Slope	(intercept)10^6, M	K_{ads} x 10^{-3}, (M^{-1})
298	0.999	1.064	1.479	676.244
308	0.999	1.090	1.861	537.253
318	0.999	1.100	2.098	476.624
328	0.999	1.156	2.536	394.223

AIC molecules on the Zn surface. The drop in K_{ads} values with temperature (Table 6) indicates a decrease in the adsorptive ability due to the desorption of AIC from Zn surface at the higher temperature.

Adsorption thermodynamic parameters

The standard free energy of adsorption, $\Delta G°_{ads}$, can be calculated from the values of the adsorption equilibrium constant, K_{ads} (Table 6), according to the equation [32]:

$$K_{ads} = \frac{1}{55.5}\exp\left(\frac{-\Delta G^{\circ}_{ads}}{RT}\right) \quad (11)$$

where 55.5 represents the molar concentration value of H_2O in mol/L and R is the universal gas constant. The negative sign of ΔG°_{ads} confirms the spontaneity of the adsorption process. Generally, when the values of ΔG°_{ads} reach -40 kJ mol^{-1} or more negative

suggest the chemical adsorption process. In case of $\Delta G°_{ads}$ = -20 kJ mol^{-1} or less negative will confirm the physical adsorption [33, 34]. The calculated values of $\Delta G°_{ads}$ (Table 7) were found to be - 57.11, - 44.07, - 45.19, - 45.19 and - 46.09 kJ mol^{-1} at 25, 35, 45, 55°C, successively. The obtained values of $\Delta G°_{ads}$ proved that AIC inhibitor is easy to adsorb on zinc surface according to chemical adsorption process. From the other point of view, the increase in the activation energy, E_a, with AIC inhibitor concentration indicates two types of interactions (chemisorption and physisorption) are involved in the inhibition process [49].

Adsorption thermodynamic parameters are employed to elucidate the adsorption behavior of AIC on Zn surface. The standard enthalpy of adsorption ($\Delta H°_{ads}$) can be calculated from Van't Hoff equation [48].

$$\frac{d\ln K_{ads}}{dT} = \frac{\Delta H°_{ads}}{RT^2} \quad (12)$$

The indefinite integration of Eq. 12 can give [49]:

$$\log K_{ads} = -\left(\frac{\Delta H°_{ads}}{2.303RT}\right) + \text{constant} \quad (13)$$

The values of log K_{ads} are plotted against T^{-1}, (Fig. 9), to give a straight-line relation, with a slope equal to - $\Delta H°_{ads}$/2.303R. The value of $\Delta H°_{ads}$ is found to be -3.92 kJ/mol (Table 7). Actually, when $\Delta H°_{ads} > 0$, an endothermic adsorption process; the chemical adsorption process is predominant. On the other hand, for $\Delta H°_{ads} < 0$, an exothermic adsorption process could be attributed to physical adsorption, chemical adsorption or a mixture of both processes [50]. The negative sign of the obtained $\Delta H°_{ads}$ indicates the exothermic nature of adsorption of AIC on Zn surface in HCl. From another side, the value of enthalpy is < 41.8 kJ mol^{-1}, which confirms that the adsorption of AIC on Zn surface is a combination of physisorption and chemisorption types, i.e. a mixed type [43, 49].

The standard adsorption of entropy, $\Delta S°_{ads}$, can also be obtained from the following equation [50, 51]:

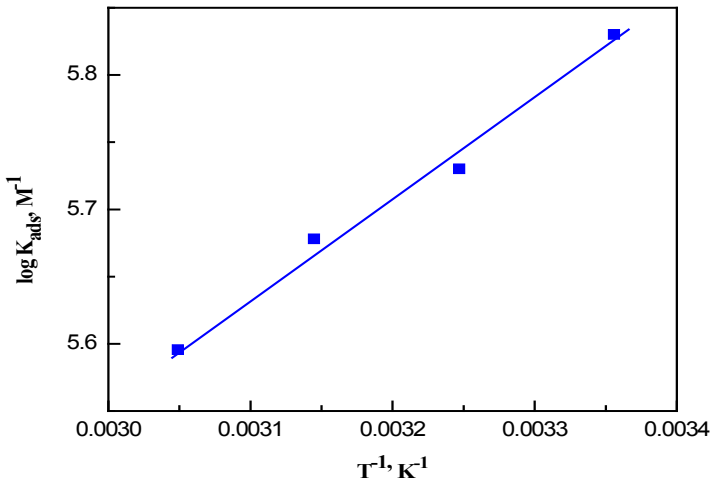

Fig. 9. Variation of log K_{corr} against T^{-1}, for Zn in 0.5 M HCl devoid of and containing different concentrations of AIC.

TABLE 7. Adsorption parameters for AIC calculated from the Langmuir adsorption isotherm on Zn in 0.5M HCl at (288 − 328) K.

Temperature, K	$\Delta G°_{ads}$, kJ/mol	$\Delta H°_{ads}$, kJ/mol	$\Delta S°_{ads}$, J mol^{-1}K^{-1}
298	-57.71	-3.92	181
308	-44.07	-3.92	130
318	-45.19	-3.92	129
328	-46.09	-3.92	128

$$\Delta S^{\circ}_{ads} = \left(\frac{\Delta H^{\circ}_{ads} - \Delta G^{\circ}_{ads}}{T} \right) \quad (14)$$

The values of ΔS°_{ads} can be calculated and collected in Table 7. The positive values of ΔS°_{ads} suggest that adsorption process is linked with a rise in the disorder of the system and this case may be due to the adsorption of only one inhibitor molecule by desorption of more than one water molecule [52].

Surface morphology

Scanning electron microscope study has been used to examine the surface of some corroded Zn samples to understand the surface properties and morphology during the of zinc surface after polishing using different grades of emery papers (Fig. 10 A). The SEM micrograph for zinc surface after immersion for a period of 1hr in 0.5 M HCl solution devoid of and containing 1x 10^{-5} M AIC inhibitor are shown in Fig. 10 B and C, respectively. The SEM micrograph of the corroded Zn sample in 0.5 M HCl solution (Fig. 10 B) shows uniform highly damaged Zn surface, which is covered by the products of corrosion. The extended corrosion area might supposedly have been created from smaller pits prolonged evenly laterally, as well as, internally so that the large attacked area is formed. In contrast, the presence of the AIC inhibitor clarified less damage surface with some numbers of pits on zinc surface (Fig. 10 C). Therefore, the existence of AIC inhibitor decreased the rate of corrosion of zinc in HCl.

Inhibition mechanism

The inhibition effect 5-amino-4-imidazolecarboxamide (AIC) towards Zn/HCl interface is supposed to be related to the molecule adsorption through the free electron pairs located on N and O atoms of AIC inhibitor molecules interface to form a defensive film. The formed inhibitive film protects the Zn surface from the aggressive effect of HCl. The adsorption process includes the replacement of H_2O_{ads} from the zinc metal surface in the aqueous phase by AIC molecules, AIC_{aqs}.

$$AIC_{aq} + x\,H_2O_{ads} \longleftrightarrow AIC_{ads} + x\,H_2O_{aq} \quad (15)$$

where x represents the number of H_2O_{ads} substituted by one molecule of AIC_{ads}. AIC_{ads} molecules can adsorb on the Zn surface via the free electrons pairs located on one O atom and four N atoms without ignoring the effective conjugated role of the π-electrons system in the molecule, confirming chemical adsorption mechanism [53].

From another point of view, the AIC inhibitor molecules are suggested to be represented by the protonated form in presence HCl aqueous solutions $[HAIC]^+$ The equilibrium between the cationic and neutral form of AIC forms can be represented by:

$$AIC + HCl \longleftrightarrow [HAIC]^+ + Cl^- \quad (16)$$

Generally, the surface of zinc metal is considered to carry a positive charge in acid solutions [48], which assist the formation of $ZnCl^-_{ads}$ on the metallic surface. An immoderate negative charge is formed on Zn surface towards the solution interface, which facilitates the adsorption of protonated inhibitor molecules, $[HAIC]^+$, onto the metal zinc surface according to physical adsorption model reducing the corrosion process.

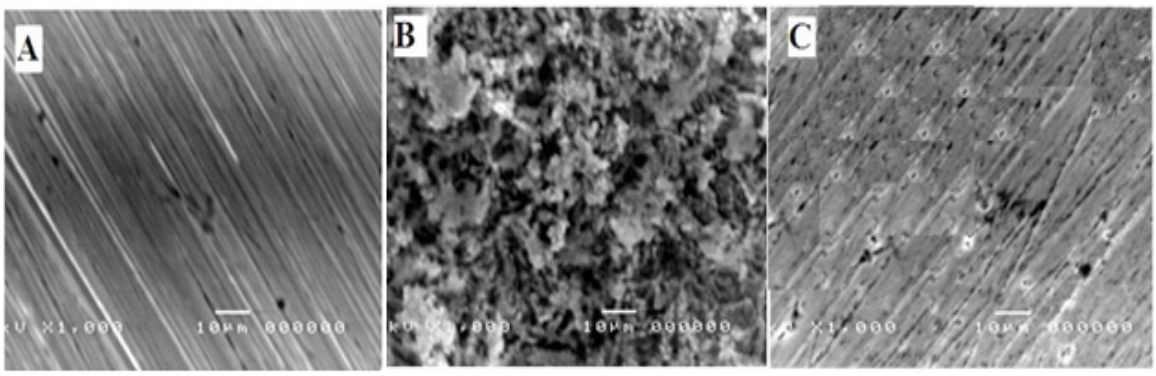

Fig. 10. SEM micrographs of Zn surface (A) polished and after inundation in (B) 0.5M HCl and (C) in 0.5M HCl + 1x10^{-5} M AIC inhibitor, for a period of 1 hr, at 25 °C.

Conclusions

Different chemical and electrochemical techniques were used to study the corrosion of zinc and H_2 production in 0.5 M HCl in the absence and presence of different concentrations of 5-amino-4-imidazolecarboxamide (AIC). The experimental data revealed the following conclusion:

1. The rates of zinc corrosion and H_2 production were found to increase with the inundation time and the solution temperature.
2. Different additions of 5-amino-4-imidazolecarboxamide decrease the rates of zinc corrosion and H_2 production as indicated by the different experimental techniques.
3. Polarization data indicated that 5-amino-4-imidazolecarboxamide acted as a mixed inhibitor inhibiting both the anodic and cathodic reactions.
4. The inhibition process was based on the mechanism of adsorption of the inhibitor molecules on the metal surface through the free electrons of O atom and N atoms besides the role controlled by the π-electrons of the conjugated double bonds system.
5. The inhibition efficiency is increased with increasing inhibitor concentration and decrease with the temperature.
6. The adsorption process is a mixed-type including the physical and chemical processes according to Langmuir isotherm.

Acknowledgment

The author gratefully acknowledges the approval and support this research study by the grant number S-0245-1437 from the deanship of science research at Tabuk University, Tabuk, K.S.A.

References

1. Abootalebi, O., Kermanpur, A., Shishesaz, M. R., Golozar, M. A., Optimizing the electrode position in sacrificial anode cathodic protection systems using boundary element method, *Corros. Sci*., **52,** 678-687 (2010).
2. Manov, S., Noli, F., Lamazouere, A. M., Aries, L., Surface treatment for zinc corrosion protection by a new organic chelating reagent, *J. Appl. Electrochem*., **29**, 995-1003 (1999).
3. Wang, F., Yu, F., Wang, X. Chang, Z., Fu, L., Zhu, Y., Wen, Z., Wu, Y., Huang, W. ACS *Appl. Mater. Interfaces*, **14**, 9022–9029 (2016).
4. Liu, S., Han, W., Cui, B., Liu, X., Sun, H., Zhang, J., Lefler, M., Licht, S., Rechargeable Zinc Air Batteries and Highly Improved Performance through Potassium Hydroxide Addition to the Molten Carbonate Eutectic Electrolyte, *J. Electrochem. Soc*. **165**, A149-A154 (2018).
5. Sayyah, S.M., Abd El-Rehim, S.S., El-Deeb, M.M., Mohamed, S.M., Corrosion inhibition of aluminium with a series of aniline monomeric surfactant and their analogues polymers in 0.5 M HCl solution, *Egypt. J. Chem.* **55**, 583– 602 (2012).
6. Fekry, A.M., Hussein, M.S., Electrochemical corrosion behavior of nano-coated Ti-6Al-4V Alloy by a novel chitosan nanoparticles/silver nanoparticles in artificial saliva solution, *Egypt. J. Chem.* **61** , 747-758 (2018).
7. Abd El Wanees, S., El Basiony, N. M., Al-Sabagh, A. M., Alsharif, M. A., Abd El Haleem, S. M., Migahed, M.A., Controlling of H_2 gas production during Zn dissolution in HCl solutions, *J. Mol. Liq*., **248**, 943-952 (2017).
8. Kowsari, E., Arman, S. Y., Shahini, M. H., Zandi, H., Ehsanie, A., Naderi, R., Pourghasemi Hanza, A., Mehdipour, M., In situ synthesis, electrochemical and quantum chemical analysis of an amino acid-derived ionic liquid inhibitor for corrosion protection of mild steel in 1M HCl solution, *Corros. Sci*., **112**, 73-85 (2016).
9. Mahdavian, M., Bagha, A., T., Alibakhshi, E., Ashhari, S., Palimia, J. M., Farashi, S., Javadian, S., Ektefa, F., Corrosion of mild steel in hydrochloric acid solution in the presence of two cationic gemini surfactants with and without hydroxyl substituted spacers, *Corros. Sci*., **137,** 62-75 (2018).
10. Li Zhou, Yan-Li Lv, Yong-Xu Hu, Jin-Hui Zhao, Xin Xi, Xiao Li, Experimental and theoretical investigations of 1,3,5-tris(4-aminopheno- xy) benzene as an effective corrosion inhibitor for mild steel in 1 M HCl, *J. Mol. Liq*., **249**,179-187 (2018).
11. Njoku, D. I., LI, Y., Lgaz, H., Ougiz, E.E., Dispersive adsorption of Xylopia aethiopica constituents on carbon steel in acid-chloride medium: A combined experimental and theoretical approach, *J. Mol. Liq.,* **249**, 371-388 (2018).
12. Popova, A., Temperature effect on mild steel

corrosion in acid media in presence of azoles, *Corros Sci.*, **49**, 2144-2158 (2007).

13. Granese, S. L., Rosales, B. M., Oviedo, C., Zerbino, J. O., The inhibition action of heterocyclic nitrogen organic compounds on Fe and steel in HCl media, *Corros. Sci*., **33**, 1439-1453 (1992).

14. Subramanian, G., Balasubramanian, K., Sridhar P., Temperature effect on mild steel corrosion in acid media in presence of azoles, *Corros. Sci*., **30**, 1019-1023 (1990).

15. Gopi, D., Sherif, El-Sayed M., Surendiran, M., Jothi, M., Kumaradhas, P., Kavitha, L., Experimental and theoretical investigations on the inhibition of mild steel corrosion in the ground water medium using newly synthesised bipodal and tripodal imidazole derivatives, *Mater. Chem. Phys*., **147**, 572-582 (2014).

16. El-Haddad, M. N., Fouda, A.S., Electroanalytical, quantum and surface characterization studies on imidazole derivatives as corrosion inhibitors for aluminum in acidic media, *J. Mol. Liq*., **209**, 480-486 (2015).

17. Singh,A., Ansari, K.R., Kumar, A., Liu, W., Chen Song song, Yuanhu Lin, Electrochemical, surface and quantum chemical studies of novel imidazole derivatives as corrosion inhibitors for J55 steel in sweet corrosive environment, *J. of Alloys Comp*., **712**, 121-133 (2017).

18. Ghanbari, A., Attar, M. M., Mahdavian, M., Corrosion inhibition performance of three imidazole derivatives on mild steel in 1M phosphoric acid, *Mater. Chem. Phys*., **124**, 1205-1209 (2010).

19. Stupnisek-Lisac, E., Kasunic, D., Vorkopic-Furac, J., Imidazole derivatives as corrosion inhibitors for zinc in hydrochloric acid. *Corrosion*, **51**, 676-681(1995).

20. Bereket, G., Öğretir, C., Yurt, A., Quantum mechanical calculations on some 4-methyl-5-substituted imidazole derivatives as acidic corrosion inhibitor for zinc, *J. Mole. Stru.: THEOCHEM,* **571**, 139-145 (2001).

21. Saleh, M., Abd El Wanees, S., Mustafa, K. S., Dihydropyridine derivatives as controllers for production of hydrogen during zinc dissolution, *Chem. Eng. Commun*. 1-15 (2018), https://doi.org/10.1080/00986445.2018.1527319

22. Abd El Wanees, S., Sada, S., Corrosion Inhibition of zinc in aqueous acidic media using a novel synthesized Schiff Base – an experimental and theoretical study, *J. Disper. Sci. Technol.* (2018) In press.

23. Abd El Aal, E. E., Abd El Wanees, S., Farouk, A., Abd El Haleem, S. M., Factors affecting the corrosion behaviour of aluminium in acid solutions. II. Inorganic additives as corrosion inhibitors for Al in HCl solutions, *Corros. Sci*., **68**, 14-24 (2013).

24. Abd El Haleem, S. M., Abd El Wanees, S., Abd El Aal, E. E., A. Farouk, A. A., Factors affecting the corrosion behaviour of aluminium in acid solutions. I. Nitrogen and/or sulphur-containing organic compounds as corrosion inhibitors for Al in HCl solutions, *Corros. Sci*., **68**, 1-13 (2013).

25. Abd El Wanees, S., Alahmdi, M. I., Abd El Azzem, M., Ahmed, H. E., 4,6-Dimethyl-2-oxo-1,2-dihydropyridine-3- carboxylic acid as an inhibitor towards the corrosion of C-steel in acetic acid, *Inter. J. Electrochem. Sci*., **11**, 3448 – 3466(2016).

26. Abd El Wanees, S., Alahmdi, M. I., Rashwan, S. M., Kamel, M. M., Abd Elsadek, M. G., Inhibitive Effect of cetyltriphenylphosphonium bromide on C-steel corrosion in HCl solution. *Inter. J. Electrochem. Sci*., **11**, 9265 – 9281 (2016).

27. Umoren, S. A., Solomon, M. M., Eduok, U. M., Obot, I. B., Israel, A. U., Inhibition of mild steel corrosion in H_2SO_4 solution by coconut coir dust extract obtained from different solvent systems and synergistic effect of iodide ions: Ethanol and acetone extracts, *J. Environ. Chem. Eng*., **2**, 1048-1060 (2014).

28. Fouda, A., S. Rashwan, S., Emam, A., El-Morsy, F. E., Corrosion inhibition of Zinc in acid medium using some novel organic compounds, *Int. J. Electrochem. Sci*., **13**, 3719 – 3744 (2018).

29. Ben Aoun, S., On the corrosion inhibition of carbon steel in 1 M HCl with a pyridinium-ionic liquid: chemical, thermodynamic, kinetic and electrochemical studies, *RSC Adv*., **7**, 36688-36696 (2017).

30. Poornima, T., Nayak, J., Shetty, A.N., 3, 4-Dimethoxy benzaldehyde thiosemicarbazone as corrosion inhibitor for aged 18Ni 250 grade maraging steel in 0.5 M sulfuric acid., *J. Appl. Electrochem*., **41**, 223 - 233 (2011).

31. Li, W. H., He, Q., Zhang, S.T., Pei, C.I., Hou, B. R., Some new triazole derivatives as inhibitors for mild steel corrosion in acidic medium, *J. Appl. Electrochem*, **38**, 289 – 295 (2008).

32. Ferreira, E.S., Giancomlli, C., Giacomlli, F.C., Spinelli, A., Evaluation of the inhibitor effect of L-ascorbic acid on the corrosion of mild steel, *Mater. Chem. Phys*., **83**, 129–134 (2004).

33. Chaitra, T. K., Shetty Mohana, K. N., Tandon, H. C., Thermodynamic, electrochemical and quantum chemical evaluation of some triazole Schiff bases as mild steel corrosion inhibitors in acid media, *J. Mol. Liq*., **211**, 1026–1038 (2015).

34. Labjar, N., Lebrini, M., Bentiss, F., Chihib, N. E., El Hajjaji, S., Jama, C., Corrosion inhibition of carbon steel and antibacterial properties of aminotris-(methylenephosphonic) acid, *Mat. Chem. Phys.,* **119**, 330–336 (2010).

35. Ashassi-Sorkhabi, H., Ghalebsaz-Jeddi, N., Hashemzadeh, F., Jahani, H., Corrosion inhibition of carbon steel in hydrochloric acid by some polyethylene glycols, *Electrochim. Acta*, **51**, 3848-3858 (2006).

36. Becke,A.D.,Density-functional thermochemistry. III. The role of exact exchange, The J. of Chemical Phys., **98**, 5648-5652 (1993).

37. Becke, A.D., Density-functional exchange-energy approximation with correct asymptotic behavior, *Phys. Rev. A*, **38**, 3098-3100 (1988).

38. Syed, J. A., Tang, S., Lu, H., Meng, X., Water-soluble polyaniline–polyacrylic acid composites as efficient corrosion inhibitors for 316SS, *Ind. Eng. Chem. Res*., **54**, 2950−2959 (2015).

39. Sekine, I., Sabongi, M., Hagiuda, H., Oshibe, T., Yuasa, M., Imahma, T., Shibata, Y., Wake, T., Corrosion inhibition of mild steel by cationic and anionic polymers in cooling water system, *J. Electrochem. Soc.,* **139**, 3167-3173 (1992).

40. Sanatkumar, B. S., Nayak, J., Shetty, A.N, Influence of 2-(4-chlorophenyl)-2-oxoethyl benzoate on the hydrogen evolution and corrosion inhibition of 18 Ni 250 grade weld aged maraging steel in 1.0 M sulfuric acid medium, *Int. J. Hydrogen Energy*, **37**, 9431–9442 (2012).

41. Abd El-Lateef, H. H. M., Abu-Dief A. M., Mohamed, M. A. A., Corrosion inhibition of carbon steel pipelines by some novel Schiff base compounds during acidizing treatment of oil wells studied by electrochemical and quantum chemical methods, *J. Mol. Struct*., **1130**, 522-542 (2016).

42. Hussein, H. M., El-Hady, M. F., Shehata, H. A. H., Hegazy, M. A., Hefni, H. H. H., Preparation of some eco-friendly corrosion inhibitors having antibacterial activity from sea food waste, *J. Surfact. Deterg*., **16**, 233–242 (2013).

43. Abd El Wanees, S., Radwan, A. B., Alsharif, M.A., Abd El Haleem, S. M., Initiation and inhibition of pitting corrosion on reinforcing steel under natural corrosion conditions, *Mater. Chem. Phys.,* **190**, 79-95 (2017).

44. Oguzie, E.E., Evaluation of the inhibitive effect of some plant extracts on the acid corrosion of mild steel, *Corros. Sci*., **50**, 2993–2998 (2008).

45. Popova A., Sokolova, E., Raicheva, S, Chritov, M., AC and DC study of the temperature effect on mild steel corrosion in acid media in the presence of benzimidazole derivatives, *Corros. Sci.,* **4**, 33 – 41(2003).

46. Tebbji, K., Faska, N., Tounsi, A., Oudda, H., Benkaddour, M., Hammouti B., The effect of some lactones as inhibitors for the corrosion of mild steel in 1 M hydrochloric acid, *Mater. Chem. Phys*., **106**, 260-267 (2007).

47. Jia-Jun Fu, Su-Ning Li, Lin-Hua Cao, Ying Wang, Lian-He Yan, Lu-De Lu., l-Tryptophan as green corrosion inhibitor for low carbon steel in hydrochloric acid solution, *J. Mater. Sci*. **45**, 979-986 (2010).

48. Morad, M. S., Inhibition of phosphoric acid corrosion of zinc by organic onium compounds and their adsorption characteristics, *J.Appl. Electrochem*., **29**, 619-626 (1999).

49. Döner, A., Solmaz, R., Özcan, M., Kardas, G., Experimental and theoretical studies of thiazoles as corrosion inhibitors for mild steel in sulphuric acid solution, *Corros. Sci*., **53**, 2902–2913 (2011).

50. Xianghong Li, Shuduan Deng, Hui Fu, Guannan Mu, Inhibition effect of 6-benzylaminopurine on the corrosion of cold rolled steel in H_2SO_4 solution, *Corros. Sci*., **51**, 620–634 (2009).

51. Hegazy, M.A., Ahmed, H.M., El-Tabei, A.S., Investigation of the inhibitive effect of p-substituted 4-(N,N,N-dimethyldodecylammonium bromide) benzylidene-benzene-2-yl-amine on corrosion of carbon steel pipelines in acidic medium, *Corros. Sci*., **53**, 671–678 (2011).

52. Hegazy, M.A., Novel cationic surfactant based on triazole as a corrosion inhibitor for carbon steel in phosphoric acid produced by dihydrate wet process, *J. Mol. Liq*., **208**, 227-236 (2015).

53. L.D., Dias, L.F.G., Albano, LG.S., Bronze-Uhle, E.S., Rangel, E.C., Graeff, C.F.O., Lisboa-Filho, P.N., Zinc oxide surface functionalization and related effects on corrosion resistance of titanium implants, *Ceram. Int*., 44 https://www-sciencedirect-com.sdl.idm.oclc.org/science/journal/02728842/44/4, 4000-4008 (2018).

تخفيف انتاج الهيدروجين أثناء تآكل الزنك في الوسط الحامضي باستخدام مركب 5- امينو4 -اميدازول كربوكساميد

صلاح عبد الونيس[2,1]، محمد عيسى الأحمدي[1]، مشاري احمد الشريف[1] و ياسمين عاطف[3]
[1]قسم الكيمياء -كلية العلوم -جامعة تبوك - السعودية.
[2]قسم الكيمياء - كلية العلوم - جامعة الزقازيق - الزقازيق - مصر.
[3]ادارة الكيمياء - القاهرة -مصر.

تتناول هذه الورقة البحثية فحص معدل إنتاج الهيدروجين أثناء تآكل معدن الزنك Zn في محاليل نصف مولارى من حامض الهيدروكلوريك في غياب ووجود كميات مختلفة من مركب5 -امينو 4- أميدازول كربوكساميد. تم استخدام تقنيات مختلفة مثل قياس الغاز، واستقطاب الجهد الديناميكي والمعاوقه الكهروكيميائية والمجهر الإلكتروني الماسح. أشارت البيانات إلى أن معدل انتاج الهيدروجين قد زاد مع الوقت ودرجة حرارة كما تم التحكم فيه مع وجود المثبط AIC العضوي أظهر التحليل الطيفي للمقاومة الكهروكيميائية أن AIC يقدم غشاءً مثبطًا يمكنه التحكم في معدل تآكل الزنك. وأشارت بيانات الاستقطاب إلى أن AIC يعمل كجزيء سطح نشط يتصرف كمثبط من النوع المختلط. تم استنباط ومناقشة الطاقة الحرة للثوابت وثوابت توازن الامتزاز والامتزاز